

https://doi.org/10.1070/QEL17266

Comparative analysis of characteristics of a supersonic cw chemical HF laser on molecular fluorine and nitrogen trifluoride

I.A. Fedorov

Abstract. **We have experimentally studied the characteristics of a supersonic cw chemical HF laser with a flat nozzle array based on a nozzle–nozzle reagent mixing scheme operating with the use of F_2–D_2–He and NF_3–D_2–He fuel compositions in an atomic fluorine generator. The active medium flow field pattern, its gas-dynamic characteristics, and the laser radiation spectrum are considered. The comparison of these characteristics has made it possible to establish a strong impact on the flow field (lasing zone length) of the chemical composition of the combustion products from the atomic fluorine generator. The gas-dynamic parameters of the active medium formed by using a NF_3–D_2–He fuel have turned out to be less acceptable in terms of the gas flow pressure recovery than in the case of F_2–D_2–He fuel, while the radiation spectrum was more preferable from the viewpoint of passing through the atmosphere.**

Keywords: *supersonic cw chemical HF laser, fluorine, nitrogen trifluoride, gas-dynamic characteristics, active medium flow pattern, laser radiation spectrum.*

1. Introduction

Analysis of the results of computational and experimental studies of energy characteristics of supersonic cw chemical HF lasers with different types of nozzle array designs, operating using various fuel compositions, which have been performed to date, gives grounds for certain optimism regarding a promising oxidiser for an atomic fluorine generator. This is NF_3 nitrogen trifluoride, a much less chemically aggressive and toxic substance compared to the 'basic' component for HF lasers – molecular fluorine F_2. When comparing the specific energy characteristics of an HF laser operating using F_2 and NF_3, it was shown that the replacement of molecular fluorine by nitrogen trifluoride with the proper organisation of the combustion process with deuterium in the combustion chamber of an atomic fluorine generator leads to a decrease in the specific energy output of the laser by no more than 23%–24% at a high combustion efficiency [1]. This circumstance gave rise to further detailed experimental studies of the characteristics of both laser radiation and the active medium of an HF laser operating with nitrogen trifluoride. It is obvious that replacing a fluorine-containing oxidiser (F_2 with NF_3) in the 'basic' F_2–D_2–He fuel composition will change not only the integral (energy), but also local gas-dynamic and spatial (flow patterns) characteristics of the active medium of an HF laser, as well as its radiation spectrum. The purpose of this work is to study the nature and extent of these changes.

I.A. Fedorov Russian Scientific Center 'Applied Chemistry', ul. Krylenko 26A, 193232 St. Petersburg, Russia; e-mail: appolo.47@mail.ru

Received 10 February 2020
Kvantovaya Elektronika **50** (11) 995–1000 (2020)
Translated by M.A. Monastyrskiy

2. Experimental conditions

The study was performed on a bench using an experimental prototype of an active medium generator of an autonomous-type supersonic HF laser with an estimated power of 5 kW, equipped with a nozzle block based on a nozzle–nozzle reagent mixing scheme with a nozzle array step (the distance between the axes of the nozzles) of 7.5 mm [2]. During these tests, the power of laser radiation and its spectrum, along with the gas-dynamic characteristics of the active medium were measured, and the flow was filmed.

To measure the laser radiation power, we used a stable two-mirror closed-type optical resonator formed by uncooled spherical mirrors-calorimeters of polished bronze with a diameter of 60 mm and a curvature radius of 5 m. The measurement technique is described in detail in work [3]. Part of the radiation coming out through a 2 mm diameter hole at the centre of one of the mirrors was directed to a high-speed scanning spectrometer (Model 501, OCLI Instruments). The spectrum was scanned in the wavelength range of 2.6–3.2 μm for 1.25 s. A photoresistor of the FSH-22-3A2 type based on gold-doped germanium was used as a radiation detector, the signal of which was amplified and recorded by electronic (Tektronix-565) and light-beam (H-117) oscilloscopes. When recording the spectra, the position of the resonator's optical axis relative to the nozzle block cutoff x_c was considered optimal from the viewpoint of attaining the maximum specific energy output (x_c^{opt} = 28 mm for the F_2–D_2–He fuel, and x_c^{opt} = 20 mm for the NF_3–D_2–He fuel). The gas-dynamic characteristics of the active medium flow (total pressure behind the direct shock wave, and static pressure) were measured by pneumometric technique using uncooled heat-resistant pressure probe-samplers that continuously moved in different flow sections parallel to the resonator's optical axis at a speed of 2 mm s^{-1}. Methods for measuring gas-dynamic characteristics and processing the results are also described in detail in work [3]. Filming of the active medium flow was performed in the direction perpendicular to the resonator's optical axis using a 1KSR-1M 'Konvas' movie camera with a frequency of 16 frames s^{-1}. All measurements of these characteristics were conducted using chemical compositions of fuels determined by conventional formulas

$$D_2 + \alpha F_2 + \psi(\alpha - 1)He + \alpha_2(\alpha - 1)H_2, \quad (1)$$

$$D_2 + (2\alpha/3)NF_3 + \psi(\alpha - 1)He + \alpha_2(\alpha - 1)H_2, \quad (2)$$

which are close to optimal in terms of attaining the maximum specific energy output [4]: $\alpha = 1.68$, $\psi = 12.6$, $\alpha_2 = 11$ (for F_2-D_2-He fuel) and $\alpha = 1.48$, $\psi = 12$, $\alpha_2 = 12$ (for NF_3-D_2-He fuel). The pressure in the combustion chamber of the atomic fluorine generator was maintained at a level of $p_c = 0.09$ MPa, while the pressure in the laser chamber (cavity) was set approximately equal to the calculated pressure $p = 5$ Torr at the outlet of the oxidising gas nozzles.

3. Pattern of the active medium flow field in the laser chamber

Figure 1 shows the kinograms of the active medium flow field recorded in the direction perpendicular to the resonator's optical axis. Without going into the details of decoding and interpretation of these kinograms, which are substantiated in [5, 6], we note that they clearly show the boundaries, length and structure of the flow (flame front configuration). The latter represents a collection of alternating dark and light zones. Dark converging (triangular) zones (*1*) correspond to the oxidising gas cooled during expansion in nozzles ($F-DF-He$ mixture), coming from an atomic fluorine generator. Extended dark zones (*2*) identify the excess cold hydrogen (secondary fuel H_2). Bright zones (*3*) (glowing front) are zones of chemical pumping reactions $F + H_2 \rightarrow HF(v) + H$ (v is the vibrational quantum number). They gradually penetrate the oxidising gas flows and reach the flow axes in a certain cross section distanced for L_{mix} from the nozzle block cutoff. The wave-like pattern at the boundaries of the reaction zones is caused by periodic shock waves that occur in a supersonic gas flow for the following reasons: deviation of the jets flowing out of the oxidising nozzles due to the gas expansion in the reaction zones; pressure mismatch in mixing supersonic jets of oxidising gas and secondary fuel; and presence of a small tilting angle of the oxidising gas jet velocity vector to the symmetry plane of the nozzle at the contour kink.

When comparing the kinograms of the flow field pattern, one can see their significant difference, in particular, a much stronger glow of the active medium formed during the NF_3-D_2-He fuel combustion (Fig. 1a). This can be explained as follows. It was shown in [5, 6] that the radiation recorded on kinograms in the visible spectrum region emerges as a result of spontaneous transitions from the upper ($v \geqslant 3$) vibrational levels of $HF(v)$ molecules pumped during both chemical reactions $F + H_2 \rightarrow HF(v) + H$ and vibrational–vibrational exchange reactions. Consequently, a stronger glow of the active medium when using the NF_3-D_2-He fuel can be explained by the presence of an additional source to pump molecules to the upper vibrational levels. Such a source can be the reaction $H + NF_3 \rightarrow HF(v) + NF_2$ which occurs in the oxidising gas flow. Its energy output, which, according to work [5], amounts to 247 kJ mol^{-1}, is quite sufficient to populate the upper ($v \geqslant 3$) levels of $HF(v)$ molecules. The large length of the glowing zone is explained by the possibility of this reaction occurring at a considerable distance from the nozzle block cutoff, since the recombination of hydrogen atoms is a very time-consuming process [7].

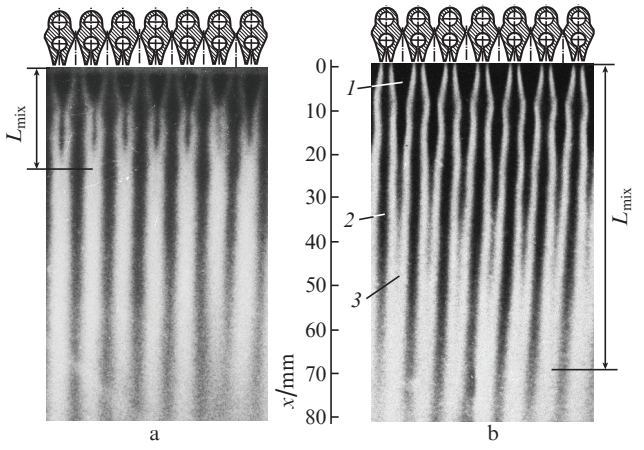

Figure 1. Kinograms of the active medium flow field of the HF laser using (a) NF_3-D_2-He and (b) F_2-D_2-He fuels: (*1*) oxidising gas jet; (*2*) secondary fuel jet; (*3*) mixing and chemical pump reaction zone.

If, according to [5], we assume that the distance at which the glowing fronts close up (conditional mixing length L_{mix}) characterises the process of mixing jets of oxidising gas and secondary fuel, it turns out that, with the optimal chemical compositions of fuels in terms of the specific laser energy output, the value of L_{mix} for the F_2-D_2-He mixture (Fig. 1b) is almost three times greater than for the NF_3-D_2-He mixture (Fig.1a). Obviously, the active zone should also be significantly expanded. This circumstance leads to a decrease in the radiation load on the resonator mirrors and in the diffraction limit of radiation divergence $\theta_{dif} \approx \lambda/L_{mix}$ (λ is the radiation wavelength).

The explanation of this fact should be sought in the difference in the parameters of the combustion products of the fuels under consideration. The higher molecular weight μ_c and lower temperature T_c of the NF_3-D_2-He fuel combustion products lead to a lower rate u_e of gas outflow from the oxidising nozzles of the same configuration, since $u_e \approx (T_c/\mu_c)^{0.5}$. Accordingly, the pump rate of the active medium is lower, and its length is shorter. This is also confirmed by the dependence of the specific energy output of the laser on the position of the resonator's optical axis x_c relative to the nozzle block cutoff. When using the F_2-D_2-He fuel, this dependence is smoother and $x_c^{opt} = 28$ mm, which is 1.4 times greater than when using the NF_3-D_2-He fuel ($x_c^{opt} = 20$ mm).

The active medium flow pattern can serve as a criterion for the adequacy of numerical models for calculating processes in a laser chamber. In particular, in work [8] it is shown that the flame front configurations, both recorded in the experiment and calculated using a mathematical model based on the complete system of Navier–Stokes equations, are in good agreement with each other. This circumstance indicates that it is possible to obtain reliable estimates not only of the integral (output power and specific energy output), but also of the local characteristics of the HF laser.

4. Gas dynamics of the active medium

Gas dynamics of the active medium flow was determined by measuring the total and static pressure profiles in various cross sections. The flow pattern was considered in a rectangular coordinate system x, y, z, the origin of which was located in the plane of the nozzle block cutoff, at its centre. The x axis was directed along the active medium flow; the y axis, along

the nozzle cutoff line; and the z axis, along the nozzle's lateral edge [2]. When measuring the total pressure, the cross sections removed by 2, 15, 30, 50, 70 and 90 mm along the x axis from the nozzle block cutoff were used as basic sections, while when measuring the static pressure, by x = 5, 11, 14, 17, 25 and 70 mm. The Mach numbers were determined using the Rayleigh formula [9, 10] for the calculated value of the adiabatic index k, based on measurements of the total pressure behind the direct shock wave P_{02} and the static pressure P_s in the active medium.

Figure 2a shows two series of profiles of the total pressure P_{02} behind the direct shock wave, which correspond to the operation of a HF laser using F_2-D_2-He and NF_3-D_2-He fuels. The locations where shock waves pass and the disturbances they introduce are clearly visible, which give the profiles a rather complex character, especially in the initial cross

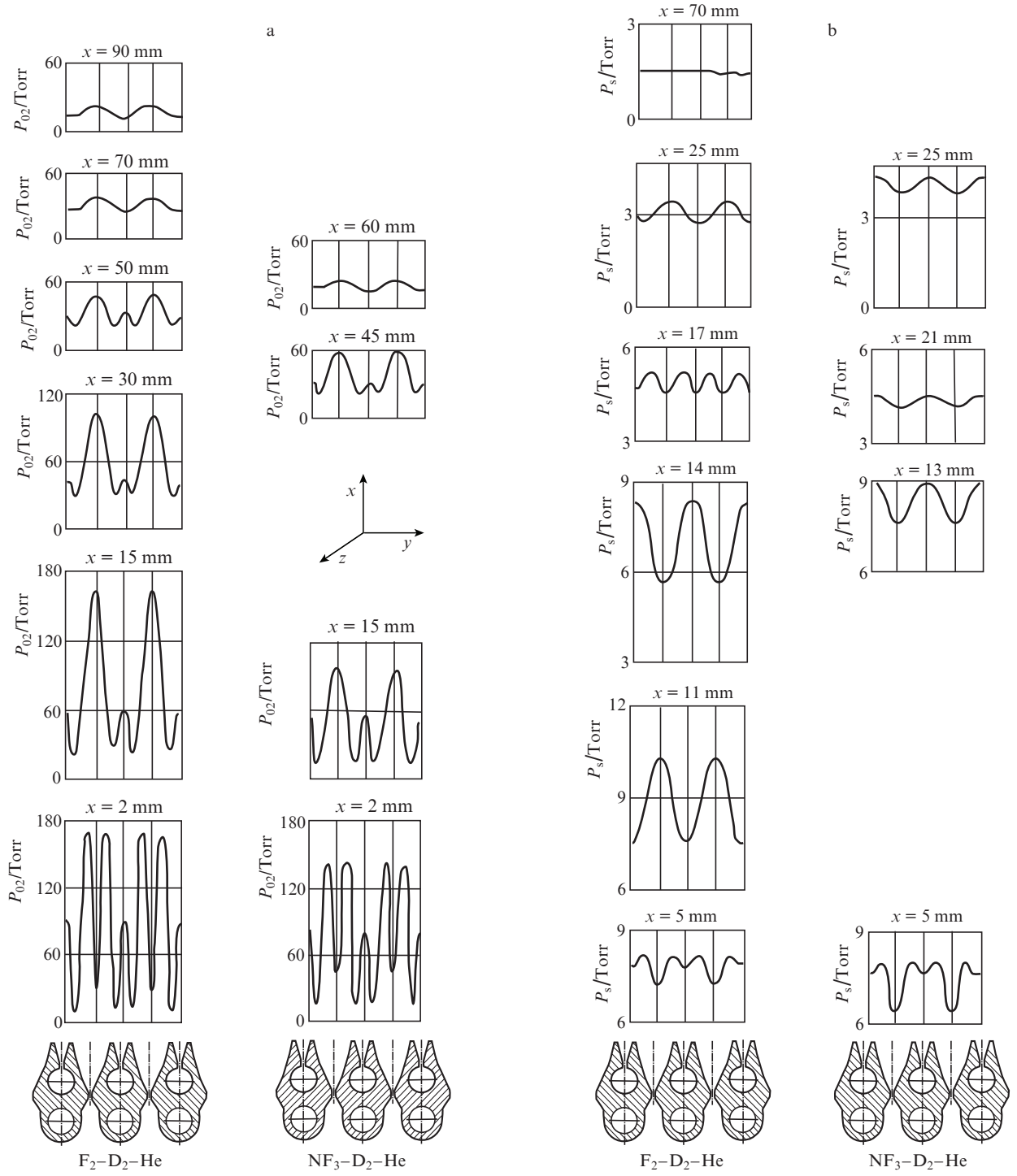

Figure 2. (a) Total pressure profiles behind the direct shock wave and (b) static pressure profiles in the active medium flow field of the HF laser using F_2-D_2-He and NF_3-D_2-He fuels. The lower part of the figure shows cross sections of the nozzle block fragments. The oxidising gas (F–DF–He mixture) flows out of the larger nozzle, and the secondary fuel (hydrogen) flows out of the smaller nozzle.

section of the flow. This character of the profiles is due to the dynamic interaction of oxidising jets and secondary fuel. As shown by the analysis of the kinograms of the active medium flow field (see Fig. 1), there is mismatch between the pressures in the output cross sections of the oxidising and hydrogen nozzles. For this reason, the boundary layer separation from the wall and the formation of separation shock waves are possible in one of the nozzles due to the compression by the separated boundary layer of the supersonic flow effluent from the nozzle.

From the shape of profiles of the total pressure P_{02} measured in the cross section $x = 2$ mm, it follows that the boundary layer separation occurs in the oxidising gas nozzles. Since this process is accompanied by a decrease in the ratio of effective nozzle expansion, flow deceleration, and an increase in pressure at the nozzle cutoff, it adversely affects the laser operation as a whole. The presence of shock waves in the active medium flow leads to a deterioration of its inverting properties due to an increase in temperature and pressure in the shock wave passage zone.

The character of profiles of the total pressure P_{02} in the cross section $x = 15$ mm indicates that the inviscid core of the flow is virtually absent in the initial section of the interaction of supersonic jets. Developed boundary layers separating from the nozzle walls close up in the immediate vicinity of the nozzle block cutoff, resulting in a completely viscous downstream flow.

The shape of the P_{02} profiles measured in subsequent flow cross sections is due to the propagation of shock waves reflected from regions near the symmetry axes of the nozzles, the dynamic interaction of the reagent jets with each other, and the effect of heat release during the chemical pump reaction. The latter process leads to significant losses of total pressure and contributes to fairly rapid smoothing of the profiles, which become virtually uniform at a distance of $x \approx 90$ mm from the nozzle block cutoff (the pressure deviation from the average level $P_{02} \approx 13$ Torr does not exceed $\pm 10\%$).

The distributions of the average values of the total pressure for the nozzles of both reagents behind the direct shock wave show a sharp decrease in the total pressure P_{02} at a distance of $x \approx 50$ mm from the nozzle block cutoff and its smooth change at larger distances. It was noted above that a sharp drop in pressure in the initial section of the flow is caused by the interaction of jets, which is accompanied by the formation of intense shock waves leading to the loss of the total energy of the flow. The heat release in the active zone and the impact of viscosity intensify this process. As the pressure increases, the total pressure changes slightly and is about 10 Torr at $x \geqslant 100$ mm. This is explained by a decrease in the intensity of shock waves downstream the flow, so that at distances of more than 100 mm it is so small that a further decrease in the total pressure is only determined by the process of the energy dissipation in the flow.

The described gas-dynamic pattern is similar when using both types of fuel. The difference lies in the greater value of the total pressure loss during the operation of the HF laser on the NF_3-D_2-He fuel (in particular, at a distance of $x = 15$ mm). This fact can be explained, on the one hand, by the additional heat release in the active zone due to the energy dissipation of reagent jets at the initial stage of their interaction and the collisional deactivation of vibrationally excited nitrogen molecules coming from the atomic fluorine generator [5], and on the other hand, by a possible change in the mixing regime of reagent jets. To confirm the latter assumption, we will refer to the results of static pressure measurements.

The profiles of the static pressure P_s in the active medium flow field are shown in Fig. 2b. It can be seen that the static pressure level P_s in the active medium formed by the NF_3-D_2-He fuel composition is slightly higher than in the medium formed by the 'basic' fuel (in particular, at distances $x = 13$ and 25 mm). This circumstance contributes to the creation of conditions for the intensification of mixing of reagent jets [11], which leads to an increase in the total pressure loss.

The distribution of the static pressure along the axes of the jets flowing from the nozzles of the oxidizing gas and secondary fuel (Fig. 3) is characterised by the presence of significant longitudinal gradients in the initial flow section due to pressure mismatch in the reagent jets. With distance from the nozzle block cutoff, the static pressure monotonically decreases, which indicates that the flow as a whole expands into the free space of the pressure chamber (where the active medium generator is located) and occurs until the pressures in the flow core and in the surrounding space become equal. Experiments have shown that this process terminates at a distance of $x \approx 100$ mm from the nozzle cutoff. It should be noted that the positions of the maxima and minima of the static pressure in the initial section of the flow fully correspond to the flow pattern revealed using kinograms (see Fig. 1). This fact convincingly testifies to the qualitative agreement between the measured and real gas-dynamic patterns of the active medium flow field.

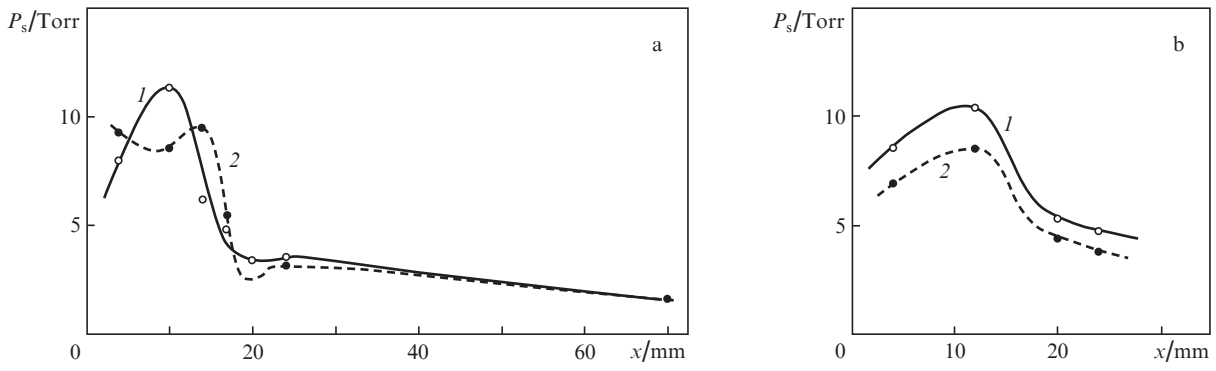

Figure 3. Distributions of static pressure in the active medium flow field of the HF laser along the axes of (*1*) oxidising gas and (*2*) secondary fuel nozzles when the laser operates on (a) F_2-D_2-He and (b) NF_3-D_2-He fuels.

The average values of the Mach numbers M in the output sections of the oxidising gas nozzles turned out to be less than the calculated values determined by the geometric degree of the nozzle expansion. In particular, on the nozzle axis when using the F_2-D_2-He fuel ($k = 1.54$), $M_{exp} = 2.93$ and $M_{theor} = 4.21$, while when using the NF_3-D_2-He fuel ($k = 1.48$), $M_{exp} = 2.65$ and $M_{theor} = 4.15$. There are two reasons for this difference. The first of them is associated with a decrease in the geometric degree of nozzle expansion under the impact of the gas flow viscosity and to burning at the nozzle edges, which leads to the penetration of disturbances upstream and mismatch between reagent pressures at the cutoff of the nozzles. The second reason is related to the gas flow specifics in the nozzles. The oxidising nozzles of the laser under study are radial (the profile of their supersonic part is formed by a circular arc). Experiments on the internal aerodynamics of such nozzles [12] have shown that it is characterised by an intense shock wave-like structure, which leads to significant losses of total pressure and, consequently, to a decrease in the Mach number.

From the viewpoint of the possibility of pressure restoration in the gas-dynamic path of an HF laser, when the waste reaction products are removed into the surrounding space, it is of great interest to know the total pressure losses, which are usually characterised by the pressure restoration coefficient $\sigma = P_{01}/p_c$ (where P_{01} is the total pressure in the incoming active medium flow). Its average values σ_m in the output section of the oxidising gas nozzles were determined from the results of measuring the pressures P_{02} and P_s. They turned out to be quite low (much less than unity): $\sigma_m = 0.27$ (for the F_2-D_2-He fuel) and 0.23 (for the NF_3-D_2-He fuel), which is a consequence of high losses of total pressure in the nozzles (higher for the NF_3-D_2-He fuel). It should be noted that the pressure restoration coefficient can be increased by increasing the mass flow rate of the secondary fuel (coefficient α_2), with the growth of which due to the pressure rise in the hydrogen jets the total pressure in the active medium flow also increases [13].

5. Laser radiation spectrum

The laser radiation spectra (ratios of the radiation power N_J on the transition lines to the levels with the rotational quantum number J to the total laser radiation power N, N_J/N) in the case of HF laser operation using F_2-D_2-He and NF_3-D_2-He fuel mixtures are shown in Fig. 4. It can be seen that there is no significant difference between them. This is quite natural, since the optimal conditions for laser operation on both fuel compositions (temperatures in the atomic fluorine generator and in the active medium), at which the spectra were recorded, are approximately the same. Both spectra have almost identical boundaries and a set of lines in the vibrational bands $v' \to v'' = 1 \to 0$ and $v' \to v'' = 2 \to 1$. From the spectrograms, eight to nine vibrational–rotational transitions in the P-branches of the $v' \to v'' = 1 \to 0$ [$P_0(7-11)$] and $v' \to v'' = 2 \to 1$ [$P_1(7-10]$ bands in the wavelength range 2.7441–2.9989 μm were identified.

It is interesting to compare these spectra with those obtained by other authors. For example, in work [14], the spectrum of an HF laser is presented, which includes transitions $P_0(4-7)$ of the band $v' \to v'' = 1 \to 0$ and transitions $P_1(4-7)$ of the band $v' \to v'' = 2 \to 1$. Noteworthy is the shift to the long-wavelength region of the spectra we have obtained (towards large values of the rotational quantum numbers J).

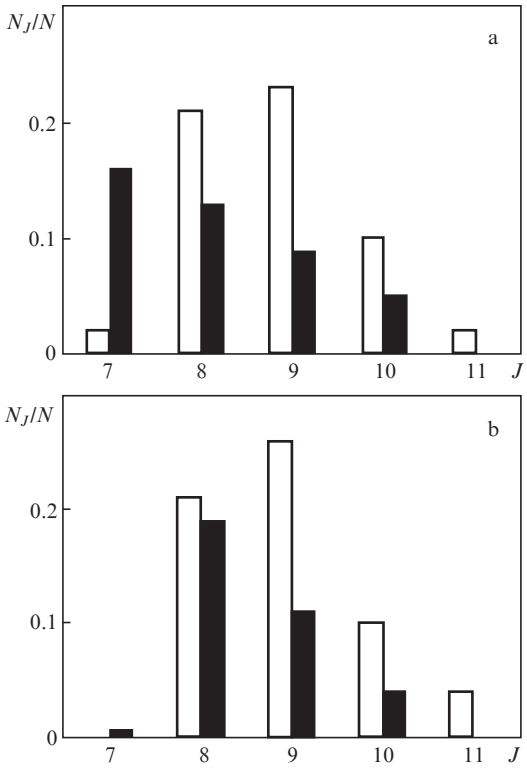

Figure 4. Emission spectra of the HF laser: (a) $F2-D_2-He$ and (b) NF_3-D_2-He fuels; N_J is the radiation power on the transition line to levels with a rotational quantum number J, and N is the total power of laser radiation; empty rectangles correspond to $v' \to v'' = 1 \to 0$ transitions, and filled ones, to $v' \to v'' = 2 \to 1$ transitions.

This, at first glance, may indicate 'overheating' of the active medium. However, to correctly interpret this fact, it is necessary to take into account that the type of the radiation spectrum is determined not only by the active medium temperature, but also by a number of other factors. They include the orientation of the resonator's optical axis relative to the nozzle block cutoff, which determines the location of the active medium region, the radiation from which is analysed, as well as the type and characteristics of the resonator that determines the lasing conditions. As shown in [15, 16], an increase in the reflection coefficients of the resonator mirrors and the degree of active medium saturation (lasing intensity) leads to a noticeable shift in the spectral power distribution towards large values of rotational quantum numbers J. In the present study, a closed-type resonator was used, resulting in lasing with a high (more than 1 kW cm^{-2}) intensity, which caused the corresponding shift of the spectra.

Regardless of the oxidiser type, the most intense transitions in the $v' \to v'' = 1 \to 0$ band are the $P_0(8, 9)$ transitions. The difference in the spectra only consists in the energy redistribution in the band $v' \to v'' = 2 \to 1$, where the maximum intensity when using molecular fluorine falls on the line $P_1(7)$, while when using nitrogen trifluoride, on the line $P_1(8)$. In the latter case, the total intensity of radiation that is weakly absorbed by the atmosphere on the $P_0(11)$ ($\lambda = 2.9103$ μm) and $P_1(8)$ ($\lambda = 2.9111$ μm) lines amounts to 24% of the total intensity (in the first case, only 15%). Within certain limits, the intensity of these lines can be controlled by varying the chemical composition of the active medium (coefficients α, ψ, and α_2), the orientation of the resonator's optical axis, and its feedback coefficient [17].

6. Conclusions

A comparative analysis of the characteristics of a prototype of a supersonic cw chemical HF laser in question, operating with molecular fluorine and nitrogen trifluoride, has shown the following.

Comparison of patterns of the active medium flow fields in the laser chamber (cavity) of a supersonic HF laser operating with F_2-D_2-He and NF_3-D_2-He fuel mixtures demonstrates the difference in the gas flow dynamics (geometry of characteristic flow regions) and the processes occurring in the cavity (glow intensity in the visible spectrum region). It turned out that the conditional mixing length, which characterises the process of mixing jets of oxidising gas and secondary fuel, for the NF_3-D_2-He mixture is three times less than that for the F_2-D_2-He mixture. This circumstance should lead to a decrease in the active zone length, as well as to an increase in the radiation load on the resonator mirrors and in the diffraction limit of the radiation divergence. This indicates a strong effect on the flow field of the chemical composition of combustion products coming from the atomic fluorine generator.

Analysis of the gas dynamics of the active medium of the HF laser under study revealed its reduced quality. Shock waves in the flow and flow separation in the oxidising gas nozzles have a negative effect on the laser energy. Significant losses of the total pressure in the radius nozzles and the nature of its change in the longitudinal direction indicate unsatisfactory gas dynamic characteristics of both active media. Moreover, the parameters of the active medium formed when using the NF_3-D_2-He fuel are less acceptable from the viewpoint of restoring the gas flow pressure when evacuating combustion products using an ejector.

As for the spectral characteristics of HF laser radiation, its spectrum when using the NF_3-D_2-He fuel is more preferable in terms of radiation transmission through the atmosphere, since the total intensity of radiation weakly absorbed by the atmosphere is almost 10% higher than when using the 'basic' fuel.

Thus, the choice of a fluorine-containing oxidiser for an atomic fluorine generator of an HF laser should obviously be based on energy and spectral characteristics of radiation, spatial and gas-dynamic characteristics of the active medium, taking into consideration the method of basing the laser installation (the necessity of a system for gas flow pressure restoration and the problem of laser radiation passage through the atmosphere).

Acknowledgements. The author considers it his duty to express gratitude to V.K. Rebone and N.E. Tret'yakov for their assistance in conducting experiments and measuring spectra.

References

1. Fedorov I.A. *Quantum Electron*., **50**, 157 (2020) [*Kvantovaya Elektron*., **50**, 157 (2020)].
2. Fedorov I.A. *Quantum Electron*., **49**, 735 (2019) [*Kvantovaya Elektron*., **49**, 735 (2019)].
3. Fedorov I.A. *Nepreryvnye khimicheskie lazery na rabochikh molekulakh ftoristogo vodoroda i ftoristogo deyteriya* (Continuous Chemical Lasers Based on Working Molecules of Hydrogen Fluoride And Deuterium Fluoride) (St. Petersburg: Baltic State Technical University, 1994) Book 2.
4. Fedorov I.A. *Nepreryvnye khimicheskie lazery na rabochikh molekulakh ftoristogo vodoroda i ftoristogo deyteriya* (Continuous Chemical Lasers Based on Working Molecules of Hydrogen Fluoride And Deuterium Fluoride) (St. Petersburg: Baltic State Technical University, 1994) Book 1.
5. Driskoll R.J., Trigay G.W. *AIAA J*., **21**, 241 (1974).
6. Varwig R.L. *AIAA J*., **12**, 1448 (1974).
7. Basov N.G., Galochkin V.T., Kulakov L.V., Markin E.P., Nikitin A.I., Oraevsky A.N. *Sov. J. Quantum Electron*., **1** (4), 348 (1971) [*Kvantovaya Elektron*., (4), 50 (1971)].
8. Egorov Yu., Rotinian M.A., Strelets M.Kh., Shur M.L., in *7th Int. Conf. on Numerical Methods in Thermal Problems*. Ed by R.W. Lewis, J.H. Chin, G.M. Homsy (Swansea, UK: Pineridge Press, 1991) Vol. VII, Pt. 2, p. 1188.
9. Spencer D.J., Varwig R.L. *AIAA J*., **11**, 1000 (1973).
10. Gorlin S.M., Slezinger I.I. *Aeromekhanicheskie izmereniya: Metody i pribory* (Aeromechanical Measurements. Methods and Devices) (Moscow: Nauka, 1964).
11. Shackleford W.L., Witte A.B., Broadwell J.E. *AIAA Paper*, No. 640 (1973).
12. Ktalkherman M.G., Malkov V.M., Ruban N.A. *Issledovanie rabochego protsessa gazodinamicheskikh i khimicheskikh lazerov* (Study of the Operating Process of Gas-Dynamic and Chemical Lasers). Ed. by V.K. Baev (Novosibirsk: Izd-vo IPTM SB USSR Acad. Nauk, 1979).
13. Fedorov I.A., Rotinyan M.A., Krivitskii A.M. *Quantum Electron*., **30**, 1060 (2000) [*Kvantovaya Elektron*., **30**, 1060 (2000)].
14. Kwok M.A., Giedt R.R., Gross R.W.F. *Appl. Phys. Lett*., **16**, 386 (1970).
15. Schulman E.R., Burwell W.G., Meinzer R.A. *AIAA Paper*, No. 74 (1974).
16. Sentman L.H., Nayfeh M.H., Renzoni P. *AIAA Paper*, No. 9 (1985).
17. Fedorov I.A., Maksimov Yu.P., Zhevlakov A.P. *Opt. Spektrosk*., **110**, 674 (2011).